

Green Synthesis AgO: Ag-NPs from Plant Extract as Reduction Agent and Antibacterial Applications

Baraa Kasim Mohammed^{1*} and Bayda Khalaf Jabbar²

¹Department of Forensic, College of Science, Al-Karkh University of Science, Baghdad, Iraq

²Al-Nahrain University, College of Science, Department of Chemistry, Baghdad, Iraq

*Corresponding author (e-mail: dr.baraa.kasim@kus.edu.iq)

In the present study, silver oxide (AgO: Ag-NPs) nanoparticles were synthesized via a green method utilizing extracts of plant material (*Nepeta cataria*). The color transformation, from light green to dark brown, indicated the successful reduction of silver ions and the formation of nanoparticles. The synthesized nanoparticles were characterized using several techniques, such as UV-Visible spectroscopy, X-ray Diffraction (XRD), Raman spectroscopy, field emission Scanning Electron Microscopy (SEM), and Fourier Transform Infrared Spectroscopy (FTIR). The synthesized AgO NPs were tested as antibacterial material against selected pathogenic bacterial strains. According to the results, silver oxide nanoparticles were synthesized as the major content AgO NPs, and a lesser content was Ag₂O NPs with Ag NPs via green methods hold potential for biomedical applications, including as anti-skin cancer agents. This potential application necessitates further investigation through comprehensive clinical studies.

Keywords: Green synthesis; AgO: Ag-NPs, *Nepeta cataria*, aggregation, antibacterial

Received: September 2025; Accepted: November 2025

The growing environmental challenges facing the planet have highlighted the urgent need for sustainable and eco-friendly solutions, particularly in the fields of energy, environmental conservation, and the removal of harmful viruses or bacteria. [1]. The synthesis of inorganic nanoparticles for various applications is a rapidly evolving area of research. Physical and chemical synthesis methods are often associated with several limitations, including high costs, the use of toxic chemical reagents, the need for sophisticated equipment, and strict reaction conditions, as well as substantial consumption of time and energy [1]. In this context, economical and biocompatible approaches have gained considerable importance in the fields of material science and nanotechnology [2], which have significantly advanced the development of efficient materials for the synthesis of macro-, micro-, and nano-scale compounds through environmentally responsible processes [3]. Synthesis and applications of nanomaterials represent the main innovative and rapidly evolving disciplines, which have shown remarkable potential in life sciences, particularly in biomedicine and biotechnology [4]. Among the various strategies for nanoparticle (NP) with mixture phase metal/metal oxide nanoparticle's M/MO-NPs,[5] the use of living organic ingredients such as plants by plant extracts derived from leaves, stems, fruit peels, seeds, and other parts has emerged as a widely adopted, green alternative [6]. Many plants have the innate ability to accumulate metal ions and facilitate their intracellular conversion into nanoparticles [7], with plant-derived biomolecules playing a critical role in the reduction and stabilization processes [8]. Variations in the size, morphology, and physicochemical properties of the resulting

nanoparticles are often attributed to the specific reducing and capping agents present in different plant species [9]. Aligned with the goals of sustainable development and circular economy principles, numerous inorganic nanoparticles, particularly with two-phase M/MO silver nanoparticles (AgO: Ag-NPs), have been synthesized using plant-based methods [10]. These biogenic nanoparticles have demonstrated a broad spectrum of biological activities, including antioxidant, antimicrobial, cytotoxic, wound healing, and even plant-growth-promoting effects, among others [11]. Typically, the green synthesis of nanoparticles involves mixing plant extracts with metal salt solutions under controlled conditions of temperature and pH, with the initial indication of NP formation often observed through a visible color change in the reaction mixture [12], which may reduce the value of aggregations. Accordingly, the objective of the present study was to evaluate the impact of environmentally synthesized AgO: Ag-NPs on the growth and viability of selected pathogenic bacterial strains. It should be mentioned that an important benefit is that the binary composite material (M/MO-NPs) behaves more actively compared to individual M or MO with NPs identities. The presence of AgO: Ag-NPs gives the material improved release of silver ions and enhanced mechanical properties [13]. In this work, NPs were synthesized via a green method utilizing extracts of plant material. Preliminary results indicate promising antimicrobial efficacy. Based on these results, it is recommended that AgO: Ag-NPs synthesized via green methods hold potential for biomedical applications, including as anti-skin cancer agents. This potential application necessitates further investigation through comprehensive clinical studies.



Figure 1. The skim for the process of synthesizing AgO: Ag-NPs.

EXPERIMENTAL

Chemicals and Materials

The *Nepeta cataria* (catnip) plant was taken from a farm in the north of Baghdad, Iraq, and AgNO₃ was purchased from Sigma-Aldrich with more than 99% purity. The extraction process was done as we reported in our previous work [14]. Briefly, the plant was washed and dried at 40 °C for 5 h before being cut into small pieces no larger than half a centimeter. 250 mL of distilled water was used as the extraction solution when dispersing the small pieces of plant and heating at 80 °C with stirring for 1 h. Then separated the undissolved suspension was separated from the extraction solution using filter paper. The aqueous solution of silver nitrate was prepared by dissolving 16.98 grams of silver nitrate in 100 mL of distilled water, before dilution to 1 mm. The extraction solution (5 mL) of plant extract was added to 95 mL of a 1 mM silver nitrate solution, and the mixture was kept in dark containers to prevent light-induced reactions for 5 days. The mixture was separated by centrifugation at 5,000 rpm for 15 minutes to eliminate precipitation material, then washed with deionized water before drying for 3 h. At 80 °C., all the steps of this work are represented by Figure 1, which starts from the extraction process and ends with application as antibacterial, in addition to passing by synthesis and characterization.

Characterization

Ultraviolet-visible spectrophotometry was used to determine the optical properties of AgO NPs by a V-630 UV-vis Spectrophotometer (Jasco, Japan) with a scan wavelength range of 200-800 nm. Functional groups for the synthesized material were determined by Fourier transform infrared spectroscopy (FTIR) (Shimadzu), with a range of wave numbers (500-4000 cm⁻¹), and 8 cm³ for resolution within potassium

bromide. Atomic Force Microscope (AFM) A thin sample of the synthesized material (silver nanoparticles/ ethanol) (100 μL) was prepared by depositing on a glass slide and left to dry for 10 minutes. The phase, particle size, and characterization of the crystalline metallic AgO NPs were analyzed by X-ray diffraction with (XRD; D8ADVANCE, Bruker). The morphology was tested by scanning electron microscopy (FE-SEM, JSM-6160). The Raman spectroscopy (Senterra II) was used to identify physical and chemical properties of materials to characterize the nature of bonding. The laser power used was 1 milliwatt, and the integration time was 5 seconds.

Antibacterial Activity

This study examines the antibacterial activity of AgO nanoparticles prepared in this research against antibiotic-resistant bacteria; we chose different types of bacteria, both of which are:

Gram-negative: *Staphylococcus aureus* (S.a) and *Streptococcus faecalis* (S.f), the other types were **Gram-positive:** *E. coli* (E.C (and *Acibetobacter baumannii*(A.B). According to the project, to ensure precision and minimize experimental errors, each concentration was tested three times. The procedure required the transfer of 0.1 ml of a standard bacterial suspension (1.5×10^8 colony-forming units/ml), corresponding to a 0.5 McFarland standard. for each isolate, along with 0.1 mL of different concentrations (50%, 75%, and 100%) of the prepared extract and silver oxide nanoparticles (AgO NPs), into sterile test tubes. Following 15-minute incubation at 37 °C, the contents were transferred onto sterile Muller-Hinton Agar plates, which were processed and distributed evenly using a sterile dispenser [15]. All plates were incubated at a temperature of 37 °C for 24 hours. The antibacterial activity was evaluated by counting the number of bacterial colonies and comparing the results with a control group.

RESULTS

As illustrated, the supposed synthesis AgO-NPs nanoparticles exhibit significant absorption near the visible light range when Figure 2a reports broad and weak peaks starting from 330-380 nm, which are related to high agglomeration of Ag₂O-NPs and AgO-NPs [16]. This phenomenon occurs due to the production of Ag nanoparticles with AgO NPs, which shifts the absorbance at the UV-region from 280 nm to 321 nm and enhances the resonance between the electromagnetic field and the collective oscillation of electrons on the surface of the nanomaterial [17]. Figure 2b refers to Raman spectroscopy, which shows the detected peaks at 223, 310, 1356, and 1582 cm⁻¹. Since the Raman technique is sensitive [18] to the element aggregations of Ag and AgO-NPs, the peak maximum intensity at 310 cm⁻¹ [19] Raman shift for Ag present in AgO NPs, and less intense peaks at 223, 1356, and 1582 cm⁻¹.

Figure 2c shows the results of the FTIR spectrum of the AgO NPs, which typically include other species such as Ag-NPs and may include

Ag/AgO and Ag₂O [20], and that was confirmed with UV-visible absorbance spectrum with XRD, and Raman spectroscopy. The nature of agglomerations and aggregations was also improved in this section, when many byproducts or remaining extraction materials for (*Nepeta cataria*), and which include by firstly broad band near 3400.57 cm⁻¹ for stretching vibrations of N-H bonds (amine or phenolic). The peaks at 2926.01 and 2854.65 cm⁻¹ are associated with C-H stretching vibrations and hydroxyl (OH), respectively, for aliphatic chains, and carboxyl (COOH) groups with weak intensity, and that is also confirmed by a distinct peak at 1739.79 cm⁻¹ for C=O stretching. These functional groups, particularly hydroxyl, carbonyl, and phenolic moieties, with small value, are known to participate in the reduction and capping of bioactive compounds during phytochemical synthesis, and that one of the main causes for agglomerations [21]. Therefore, the presence of these groups supports the potential role of the catnip plant extract as both a reducing and stabilizing agent in green synthesis processes, consistent with previous reports [22].

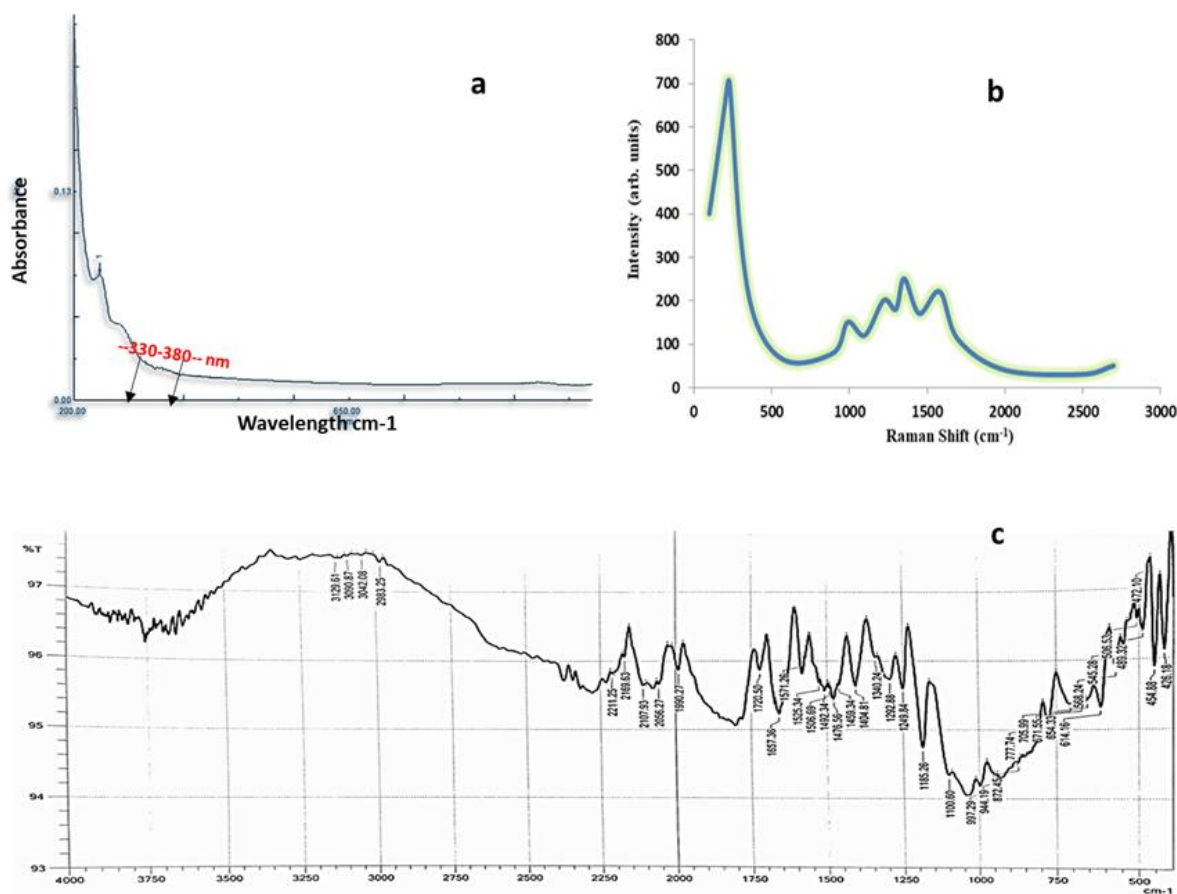


Figure 2. Spectrum for identified AgO: Ag-NPs by (a)UV-Vis spectroscopy, (b) Raman spectroscopy, and (c) IR spectrum.

According to the analysis techniques previously followed by XRD patterns in Figure 3, it should refer to an important and critical fact, which is: Ag in the Nano scale was commonly prepared and typically identified by XRD due to the ability to characterize and identify different Ag environments such as Ag₂O, AgO, Ag/Ag₂O, and Ag/AgO [23]. Figure 2 reports two types of peaks, the first group was 29.5°, 34°, and 57° with planar phase (100), (111), and (220) respectively, and that responsible for AgO NPs. The second group

was 38°, 44°, 57° and 66° refers to Ag NPs with planer phase (111), (200), (200) and (220) [Rastogi, Lori, Arunachalam, J., " Sunlight based irradiation strategy for rapid green synthesis of highly stable silver nanoparticles using aqueous garlic (*Allium sativum*) extract and their antibacterial potential, Materials Chemistry and Physics, 2011, V. 129 (1), pp. 557 - 563]. The values of peaks were estimated by Debye Scherrer's formula [24], when shown commonly range between less than 28 nm to 55.3077 nm for the mean crystallite size, as shown in Table 1.

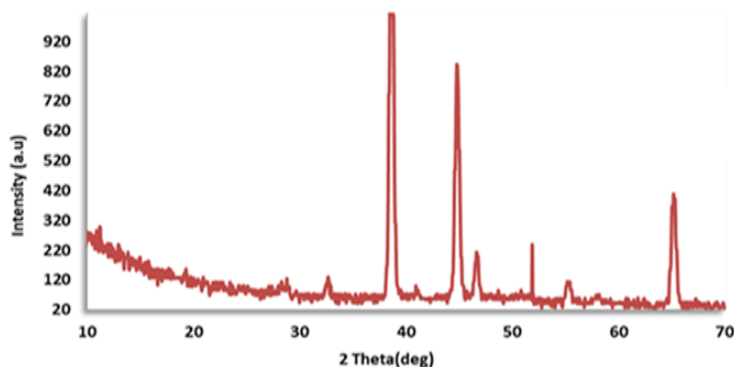


Figure 3. XRD patterns for synthesized AgO: Ag-NPs.

Table 1. Estimation and summary for FWHM and Crystallite size of the AgO: Ag-NPs.

Nano composite	Pos. [°2Th.]	Height [cts]	FWHM Left [°2Th.]	d-spacing [Å]	Rel. Int. [%]	Tip Width
	38.6109	1324.86	0.3444	2.33190	100.00	0.4133
	44.8272	792.47	0.4920	2.02192	59.82	0.5904
AgO NPs.	46.6669	159.07	0.3936	1.94641	12.01	0.4723
	55.3077	70.09	0.4920	1.66104	5.29	0.5904
	65.2007	329.26	0.4920	1.43091	24.85	0.5904
	78.2436	90.39	0.4920	1.22183	6.82	0.5904

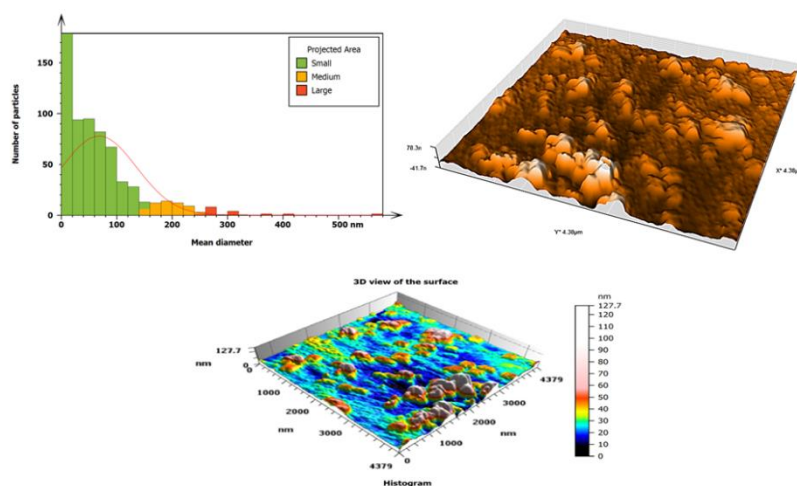


Figure 4. AFM images of Inorganic oxide silver nanoparticles. (A): Column AFM diagram for the size range of aggregation mixture Ag-NPs AgO NPs; (B): Two-dimensional; (C): Three-dimensional AFM images.

The surface morphology was examined using atomic force microscopy (AFM), which provides two-dimensional and 3D AFM images as shown in Figure 4, revealing that the existence is mostly a mixture aggregation Ag-NPs and AgO-NPs with an average particle size of approximately 98.5-96 nm.

Morphological characterization of the aggregations of AgO nanoparticles was performed using field emission scanning electron microscopy (FESEM). Figure 5 presents FESEM images of the mixture of Ag-NPs and AgO-NPs at various magnifications (100, 200 nm, and 1, 10 μm). The images reveal that the nanoparticles exhibit a predominantly spherical shape with a relatively uniform size distribution. The homogeneity with aggregation dispersion suggests that the synthesis method employed is effective and potentially superior in producing Ag/AgO nanoparticles with controlled diameters.

The Biomedical Applications

The microbial activity of the manufactured nanostructures as nanocomposites was tested against four bacteria: *Staphylococcus aureus* (*S.a*), *Enterococcus faecalis* (*S.f*), *Escherichia coli* (*E.c*), and *Acinetobacter baumannii* (*A.b*). [25] A sample of 0.06 g of the inorganic silver oxide (AgO: Ag-NPs) was taken and then dissolved in 5 ml of dimethyl sulfoxide (DMSO), and the direct inhibitory effect of inorganic (AgO: Ag-NPs) against pathogenic microorganisms was determined using the well

diffusion method under aerobic conditions [26]. As indicated in Table 2. It was observed that the levels of antibacterial activity of (AgO: Ag-NPs) at the highest concentration of nanoparticles exhibited the largest inhibition zone (30 mm). (100%) against (*S. aureus*) with (29 mm) (100%) against (*S. faecalis*) for Gram-positive bacteria, and (19 mm) (100%) against (*E. coli*) and (20 mm) (100%) against (*A. baumannii*) for Gram-negative bacteria, compared to the antibiotic used (levofloxacin), where the inhibition zone was smaller.

The results confirmed that this plant exhibits broad-spectrum antibacterial activity against several clinically significant pathogens, many of which are associated with hospital-acquired infections [27], including strains exhibiting high levels of antibiotic resistance. Additionally, *N. cataria* demonstrated effectiveness against bacteria implicated in foodborne illnesses, food poisoning, and spoilage [28]. Owing to these properties, the plant holds considerable promise in both pharmaceutical and food industries, as well as in the green synthesis of nanoparticles with antimicrobial potential. The enhanced antibacterial action observed may be attributed to structural differences in bacterial cell walls. Gram-positive bacteria, lacking an outer membrane, allow greater permeability of antimicrobial agents compared to gram-negative bacteria, which possess an outer lipopolysaccharide layer enriched with proteins that act as a barrier, limiting the penetration of harmful substances.

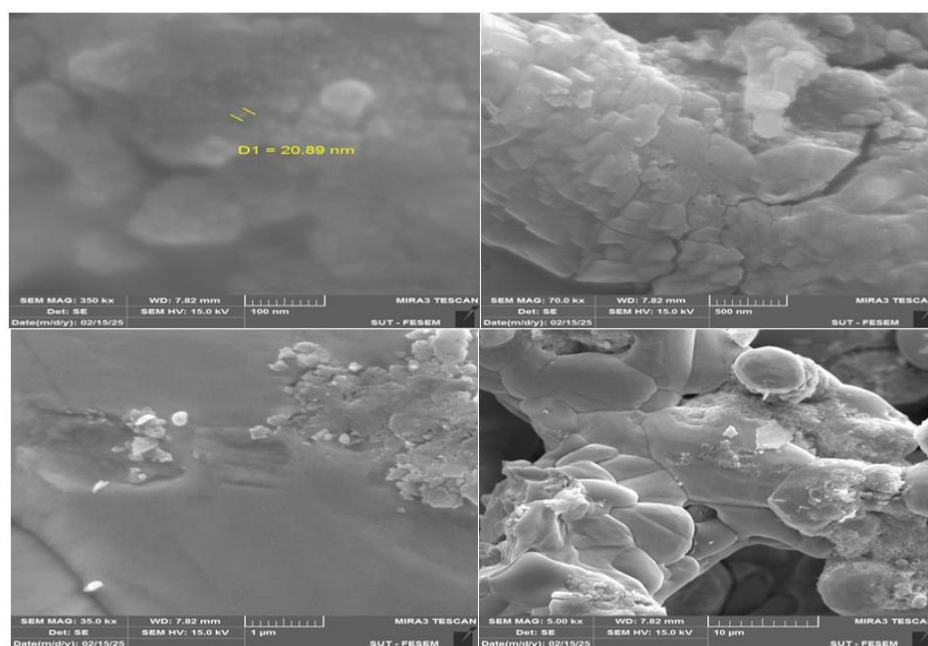


Figure 5. The FE-SEM images for Ag/AgO NPs.

Table 2. The antibacterial activity of AgO: Ag-NPs compound.

Co.50%	Co.75%	Co.100%	Levofloxacin	Name	Type Bacteria
18	28	30	16	<i>Staphylococcus aureus (S.a)</i>	Gram-positive bacteria
10	20	29	15	<i>Streptococcus faecalis (S.f)</i>	Gram-positive bacteria
14	17	19	14	<i>Escherichia coli (E.c)</i>	Gram-negative bacteria
12	15	20	12	<i>Acibetobacter baumannii (A.b)</i>	Gram-negative bacteria

DISCUSSION

In this study, the optical properties of the synthesized AgO: Ag-NPs were assessed using UV-Vis spectroscopy. The spectrum displayed a distinct absorption peak at 242 nm, which is indicative of the characteristic SPR band associated with AgO: Ag-NPs [29].

According to the UV-visible absorbance spectrum, the shift or increase in wavelength from 280 nm to more than 300 nm can be related to forming Ag NPs with AgO NPs [30]. The patterns of XRD also refer to forming AgO: Ag-NPs, and that was confirmed by Raman spectroscopy and FTIR, which showed the formation of new concoctions in addition to Ag with oxide with a variance in valence value [31].

The morphology analysis obtained from AFM and SEM shows that agglomerations exist in all images with different scales due to the polarity of oxide groups in different phases, with a maximum level for AgO and a lower level for Ag₂O [32]. The solubility and dispersion of synthesized AgO: Ag-NPs in solution, which absolutely reduce the agglomerations that created many active sites, but did not prevent the formation of aggregation. Experimentally, according to the results, the higher resistance of *Escherichia coli* and *Acinetobacter baumannii* relative to *Staphylococcus aureus* and *Streptococcus faecalis* to the antibiotics was variable with increased concentration [33]. Moreover, *N. cataria* is known to produce a diverse array of secondary metabolites, many of which have garnered significant attention due to their potent biological activities and unique chemical structures. It is also important to note that the characteristics of synthesized silver nanoparticles (AgO: Ag-NPs) can vary significantly depending on the biological source, synthesis method, and reaction conditions, leading to differences in particle size, shape, and overall functionality.

CONCLUSION

The synthesized process in this work witnessed abilities for the extraction solution to produce an active mixture for Ag with different species, such as AgO, Ag₂O, and Ag, and that absolutely enhances the

activities of the solution against specific selective bacteria in this work. The analysis process proved that the synthesized AgO: Ag-NPs is a homogeneous mixture that successfully disperses in solution and acts as an inhibitory factor against bacteria with the lowest aggregations. The current study indicates that the synthesis of inorganic silver oxide nanoparticles using wild mint extract yields effective results in their ability to inhibit the growth of both Gram-positive and Gram-negative bacteria. It has been found that nanoparticles have a greater effect on Gram-positive bacteria compared to Gram-negative bacteria in terms of the diameter of the inhibited bacteria. Furthermore, the activity of the prepared material was compared to that of the drug (Levofloxacin); the results showed a higher effectiveness of the substance compared to the effectiveness of the drug (Levofloxacin), which showed less inhibition.

REFERENCES

1. Vinukonda, A., Bolledla, N., Jadi, R., Chinthala, R., and Devadasu, V. (2025). Synthesis of nanoparticles using advanced techniques. *Next Nanotechnology*, **8**, 100169.
2. Ranjha, M., Shafique, B., Rehman, A., Mehmood, A., Ali, A., Zahra, S., and Siddiqui, S. (2022). Biocompatible nanomaterials in food science, technology, and nutrient drug delivery: recent developments and applications. *Frontiers in Nutrition*, **8**, 778155.
3. Gupta, D., Boora, A., Thakur, A., and Gupta, T. (2023) Green and sustainable synthesis of nanomaterials: recent advancements and limitations. *Environmental Research*, **231**, 116316.
4. Khan, Y., Sadia, H., Ali Shah, S., Khan, M., Shah, A., Ullah, N., Ullah, M., Bibi, H., Bafakeeh, O., Khedher, N. and Eldin, S. (2022) Classification, synthetic, and characterization approaches to nanoparticles, and their applications in various fields of nanotechnology: A review. *Catalysts*, **12**, 1386.
5. Laouini, S., Bouafia, A., Soldatov, A., Algarni, H., Tedjani, M., Ali, G. and Barhoum, A. (2021). Green synthesis of Ag/Ag₂O nanoparticles using

- aqueous leaves extracts of *Phoenix dactylifera* L. and their azo dye photodegradation. *Membranes*, **11**, 468.
6. Regolo, L., Giampieri, F., Battino, M., Armas Diaz, Y., Mezzetti, B., Elexpuru-Zabaleta, M., Mazas, C., Tutusaus, K., and Mazzoni, L. (2024). From by-products to new application opportunities: the enhancement of the leaves deriving from the fruit plants for new potential healthy products. *Frontiers in Nutrition*, **11**, 1083759.
 7. Goncharuk, E. and Zagoskina, N. (2023) Heavy metals, their phytotoxicity, and the role of phenolic antioxidants in plant stress responses with focus on cadmium. *Molecules*, **28**, 3921.
 8. Prakash, S., Gupta, R., and Deswal, R. (2023) Nanoparticle protein corona: understanding NP biomolecule interactions for safe and informed nanotechnological applications including stress alleviation in plants. *Journal of Plant Growth Regulation*, **42**, 6377–6396.
 9. Dikshit, P., Kumar, J., Das, A., Sadhu, S., Sharma, S., Singh, S., Gupta, P., and Kim, S. (2021) Green synthesis of metallic nanoparticles: Applications and limitations. *Catalysts*, **11**, 902.
 10. Agarwal, R., Gupta, N., Singh, R., Nigam, S., and Ateeq, B. (2017). Ag/AgO nanoparticles grown via time dependent double mechanism in a 2D layered Ni-PCP and their antibacterial efficacy. *Scientific Reports*, **7**, 44852.
 11. Kulkarni, D., Sherkar, R., Shirsathe, C., Sonwane, R., Varpe, N., Shelke, S., More, M., Pardeshi, S., Dhaneshwar, G., Junnuthula, V., and Dyawanapelly, S. (2023) Biofabrication of nanoparticles: sources, synthesis, and biomedical applications. *Frontiers in Bioengineering and Biotechnology*, **11**, 1159193.
 12. Suppiah, D., Julkapli, N., Sagadevan, S. and Johan, M. (2023). Eco-friendly green synthesis approach and evaluation of environmental and biological applications of Iron oxide nanoparticles. *Inorganic Chemistry Communications*, **152**, 110700.
 13. Dashtizadeh, Z. and Jookar Kashi, F. (2025) Comparison of anti-biofilm and cytotoxic activity of Ag/AgO, Ag/Ag₂O, and Ag/AgCl nanocomposites synthesized using stem, leaf, and fruit pericarp of *Prunus mahaleb* L. *Scientific Reports*, **15**, 26450.
 14. Sari, B., Yesilot, S., Ozmen, O., and Aydin Acar, C. (2025). Superior in vivo wound-healing activity of biosynthesized silver nanoparticles with *Nepeta cataria* (catnip) on excision wound model in rat. *Biological Trace Element Research*, **203**, 1502–1517.
 15. Kasim, M. (2023). Synthesis, structural characterisation and biological activity; new metal complexes derived from semicarbazone ligand, **10**, 21931.
 16. Gungure, A., Jule, L., Nagaprasad, N., and Ramaswamy, K. (2024). Studying the properties of green synthesized silver oxide nanoparticles in the application of organic dye degradation under visible light. *Scientific Reports*, **14**, 26967.
 17. Ali, I. A., Ahmed, A., and Al-Ahmed, H. (2023). Green synthesis and characterization of silver nanoparticles for reducing the damage to sperm parameters in diabetic compared to metformin. *Scientific Reports*, **13**, 2256.
 18. Jung, D., Hwang, S., Kim, H., Yun, S., Han, J., and Lee, N. (2025) Environment-controlled agglomeration in nanoporous Ag films with ultrathin silicon oxide. *Thin Solid Films*, **821**, 140683.
 19. Alnuaimi, M., Hamdan, N., Abdalraheem, E. and Aljanabi, Z. (2019). Biodegradation of malathion pesticide by silver bio-nanoparticles of *Bacillus licheniformis* extracts. *Research on Crops*, **20**, 79–84.
 20. Summer, M., Ali, S., Tahir, H., Abaidullah, R., Fiaz, U., Mumtaz, S., and Farooq, M. (2024). Mode of action of biogenic silver, zinc, copper, titanium and cobalt nanoparticles against antibiotic-resistant pathogens. *Journal of Inorganic and Organometallic Polymers and Materials*, **34(4)**, 1417–1451.
 21. Liga, S., Vodă, R., Lupa, L., Moacă, E., Muntean, D., Barbu-Tudoran, L., and Péter, F. (2025). Synthesis of Ag₂O/Ag Nanoparticles Using Puerarin: Characterization, Cytotoxicity, In Ovo Safety Profile, Antioxidant, and Antimicrobial Potential Against Nosocomial Pathogens. *Journal of Functional Biomaterials*, **16**, 258.
 22. Villagrán, Z., Anaya-Esparza, L., Velázquez-Carriles, C., Silva-Jara, J., Ruvalcaba-Gómez, J., Aurora-Vigo, E., Rodríguez-Lafitte, E., Rodríguez-Barajas, N., Balderas-León, I. and Martínez-Esquivias, F. (2024). Plant-based extracts as reducing, capping, and stabilizing agents for the green synthesis of inorganic nanoparticles. *Resources*, **13**, 70.

23. Thiruvengadam, V. and Bansod, A. (2020) Characterization of silver nanoparticles synthesized using chemical method and its antibacterial property. *Biointerface Res. Appl. Chem.*, **10**, 7257–7264.
24. Kasim, M. (2017) Kinetic Study of Adsorption for Doxycycline Drug from Aqueous Solutions by Bentonite and Activation Bentonite at Different Temperatures. *Journal of Education and Scientific Studies*, **10**, 135–150.
25. Alavi, M. and Rai, M. (2019). Recent advances in antibacterial applications of metal nanoparticles (MNPs) and metal nanocomposites (MNCs) against multidrug-resistant (MDR) bacteria. *Expert Review of Anti-Infective Therapy*, **17**(6), 419–428.
26. Abbas, A., Abdulrahman, B., and Mustafa, T. (2024). Preparation and Characterization of Silver Nanoparticles and its Medical Application against Pathogenic Bacteria. *Baghdad Science Journal*, **21**, 9.
27. Alzaareer, M., Azemi, A., Shibl, A., Sawalha, M., Alahmadi, H., Elshatarat, R., Oleimat, B., Saleh, A., Saleh, Z., and Ismail, N. (2025). Characterization of Opportunistic Bacterial Strains in Intensive Care Unit patients and Assessment of Natural Crude Extracts for Antibacterial Drugs: A Cross-Sectional Study. *Research Journal of Pharmacy and Technology*, **18**, 1268–1275.
28. Cheesman, M., Shivashakaregowda, N., and Cock, I. (2023). Bacterial foodborne illness in Malaysia: Terminalia spp. as a potential resource for treating infections and countering antibiotic resistance. *The Malaysian Journal of Medical Sciences*, **30**, 42.
29. Mohanaparameswari, S., Balachandramohan, M., Sasikumar, P., Rajeevgandhi, C., Vimalan, M., Pugazhendhi, S., Ganesh Kumar, K., Albukhaty, S., Sulaiman, G., Abomughaid, M., and Abu-Alghayth, M. (2023). Investigation of structural properties and antibacterial activity of AgO nanoparticle extract from Solanum nigrum/Mentha leaf extracts by green synthesis method. *Green Processing and Synthesis*, **12**, 20230080.
30. Abdalameer, N., Khalaph, K., and Ali, E. (2021). Ag/AgO nanoparticles: Green synthesis and investigation of their bacterial inhibition effects. *Materials Today: Proceedings*, **45**, 5788–5792.
31. Khan, A., Afzal, M., Rasool, K., Ameen, M., and Qureshi, N. (2023). In-vivo anticoccidial efficacy of green synthesized iron-oxide nanoparticles using Ficus racemosa Linn leaf extract (Moraceae) against Eimeria tenella infection in broiler chicks. *Veterinary Parasitology*, **321**, 110003.
32. Abdulrazzak, F., Abbas, A., Mohammed, M., Radhi, I., Abdullatif, A., Yaseen, H., Yas, D., and Alkaim, A. (2018). Preparation and Characterization of Silver Oxide Nanoparticles (AgNPs) and Evaluation the Ratios of Oxides. *Journal of Engineering and Applied Sciences*, **14**, 9177–9184.
33. Mikhailova, E. (2024). Green silver nanoparticles: an antibacterial mechanism. *Antibiotics*, **14**, 5.